EUROPEAN ORGANIZATION FOR NUCLEAR RESEARCH
ORGANISATION EUROPEENNE POUR LA RECHERCHE NUCLEAIRE

CERN - PS DIVISION

PS/ LP/ Note 93-40 (Tech.)

GEOMETRICAL ALIGNMENT AND TIMING OF 45° PULSE TRAIN GENERATORS

P. M. Devlin-Hill

Geneva, Switzerland
28 June, 1993

Geometrical alignment and timing of 45° Pulse Train Generators.

P.M.Devlin-Hill

CERN, CH-1211 Geneva 23

Abstract

In this paper details of the optical method of alignment of 45° pulse train generators (PTGs), based on the observation of Tolansky fringes, and used in the CLIC test facility (CTF) are given. An example of an intergrated alignment procedure and a method of ensuring correct injection are presented along with stage length calculations. The influence of beam splitter substrate wedge angle on the achievable degree of coincidence of pulses on a distant photocathode is discussed. Experimentally timing accuracies of at least 1.5ps and possibly better than 500fs, and submillimeter alignment accuracies were achieved. It is shown computationally that alignment accuracies of the order of a few μm should be achievable.

1 Introduction

A PTG is an optical system used to provide from a single laser pulse a train of pulses of equal intensity and separated by a given time interval. Such trains of pulses, with a pulse separation of one 3 GHz cycle, are required to generate the 30GHz power required for rf structure tests in the CTF. A 45° PTG is one in which an incident light pulse hits each optic it encounters at an angle of incidence of 45° and of these generators there are two types as illustrated in figures (1) and (2). The advantages of using the system illustrated in fig.(1)a, the principles according to which it may be aligned and the theoretically achievable timing accuracies have been described in some detail in reference [1]. However reference [1] reported the observation of large timing errors. These errors have now been corrected. The source was traced to the misinterpretation of injection error and subsequent inappropriate adjustment of the generator and to neglect of the group refractive index of the substrate matieral [2] in the stage length calculations. Timing accuracies of at least 1.5ps and possibly better than 500fs have been achieved.

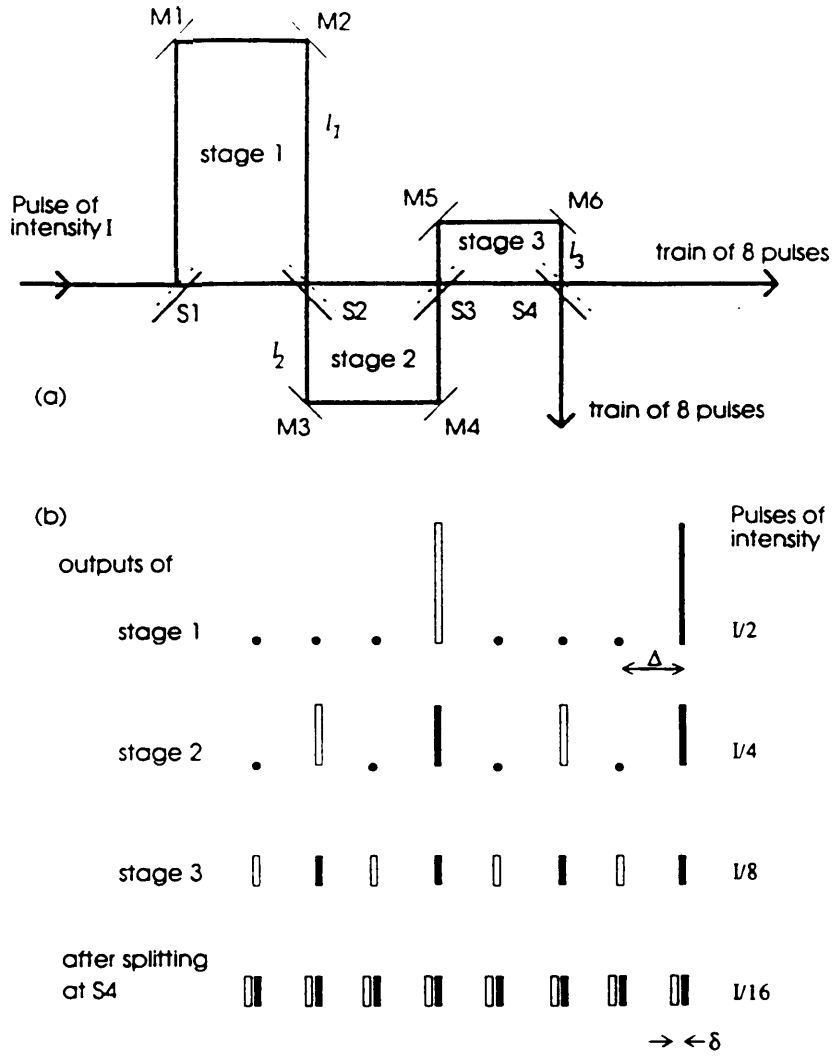

Figure 1:(a) Schematic of a 45° PTG geometry. S1 to S4 are the beam splitters, the dashed line indicating the side of the substrate on which the beam splitter coating has been deposited. M1 to M6 are high reflectivity mirrors. l_1, l_2, and l_3 are the detour lengths of stages 1, 2 and 3 respectively which together generate a train of pulse separation Δ. At S4 a delay δ determined by the substrate thickness of S4 would be introduced between the two trains of eigth. (b) Illustration of how the pulses within the train are generated.

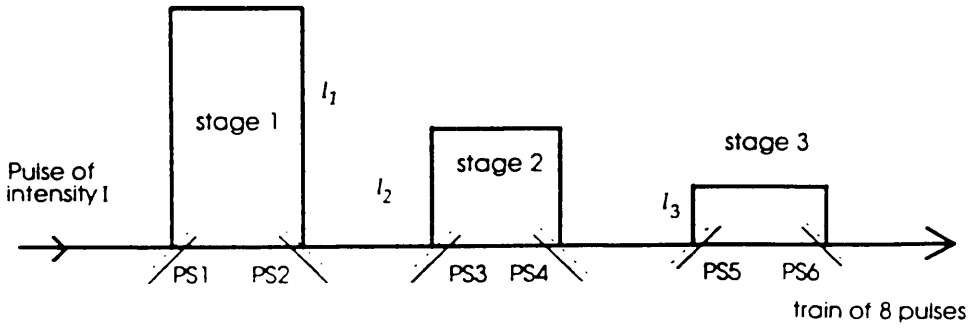

Figure 2: Geometry of 45° PTG using 45° polarizing beam splitters marked PS1 to PS6. High reflectivity mirrors and waveplates not shown.

In this note the principles according to which 45° generators may be aligned are briefly reviewed. Complete alignment of such systems is achieved in three steps;-

1. geometrical alignment
2. timing (measurement of stage lengths)
3. injection

For each step an example of an alignment procedure is given and explained. Equations giving stage length are derived and injection error and the influence of substrate wedge angle on the degree of acheivable spatial coincidence of the train pulses on a photocathode located at some distance from the PTG output discussed.

A 45° system such as that shown in figure (2) could be built for those wavelengths at which 45° polarizing beam splitters are available and may also be aligned using the techniques described here.

2 Geometrical Alignment

The principle advantage of 45° PTGs is that the optics are required to be either parallel to each other e.g. M1 with respect S1, or perpendicular to each other e.g. M1 with respect to M2, in order to provide a 180° detour, as shown in fig.(1), and therefore may be easily aligned using the technique developed by Bergman and Thompson [3]. Once aligned the distance between the optics defining the stage length can be accurately determined and correct injection of the main laser pulse acheived.

2.1 Aligning two surfaces with respect to each other

The technique of Bergman and Thompson are applied to the optics of the generator using the configuration illustrated in figure (3). In this case the axis of the diverging light coming from the pinhole source is bent through an angle of 90° using a total internal reflection (TIR) prism placed between the two surfaces to be aligned. Bergman and Thompson show, that for $d \gg s$ where d is the distance between the pinhole screen and the optic furthest from it, i.e. M2 of fig.(3), and s is the distance between the optics that α the angle between the surfaces is given by

$$\alpha = \frac{\delta s}{2d^2} \tag{1}$$

where α is in radians and δ is the displacement of the centre of the fringe system from the centre of the pinhole as shown. d and s are both measured along the alignment beam path. When the reflecting surfaces are parallel to each other and perpendicular to the axis of the alignment beam the circular Tolansky fringe pattern will be centred on the pinhole. Ford and Shaw[4] show, for the complementary fringe pattern in the transmitted light, that

$$\alpha = \frac{\delta s}{(d + l)d} \qquad (2)$$

where l is the distance between the optic furthest from the point source and the screen placed after it. All distances are measured along the alignment beam path.

When observing the fringe system in reflection all that is required to ensure that the two surfaces being aligned are both parallel to each other and perpendicular to the alignment beam is that the fringe system be aligned concentric with the illuminating point source [5]. In transmission one must ensure that the fringe system is not 'tilted'; this decribes the situation in which the inner fringes of the system are observed in their entirety but those further out appear to be 'tilted into the shadow' for example it may be that only the bottom portions of these circular fringes are observed. This tilt error between the parallel surfaces and the axis of the alignment beam is removed by adjusting the alignment of both.

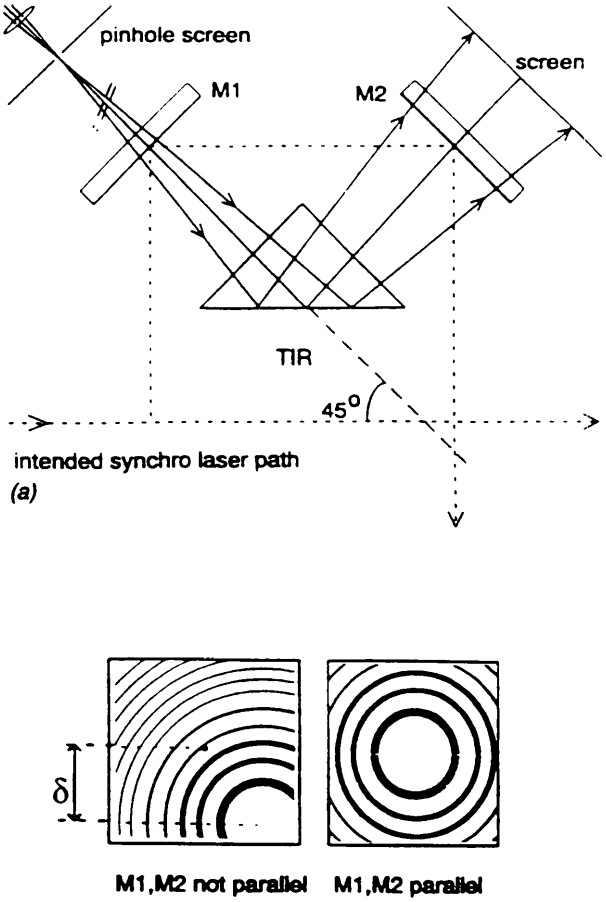

Figure 3:(a) Configuration using a total internal reflection (TIR) prism allowing the observation of Tolansky fringes between the two plane parallel reflecting surfaces of M1 and M2. Fringes will be observed in reflection on a pinhole screen or in transmission on the screen placed behind M2. Diagram not to scale. (b) Sketchs of the fringe patterns as would be observed on the pinhole screen. When the surfaces are aligned parallel to each other and perpendicular to the axis of the alignment beam the circular fringe pattern will be centered on the pinhole. Otherwise a displacement δ of the center of the fringe system from the pinhole will be observed. A complementary pattern will be observed in transmission.

2.2 Example of an intergrated geometrical alignment procedure and specification of optics

In practise the optics of the generator are mounted on carriages which slide along parallel rails as shown in figure (4). To illustrate how geometrical alignment is achieved a procedure for aligning rail (1) is presented.

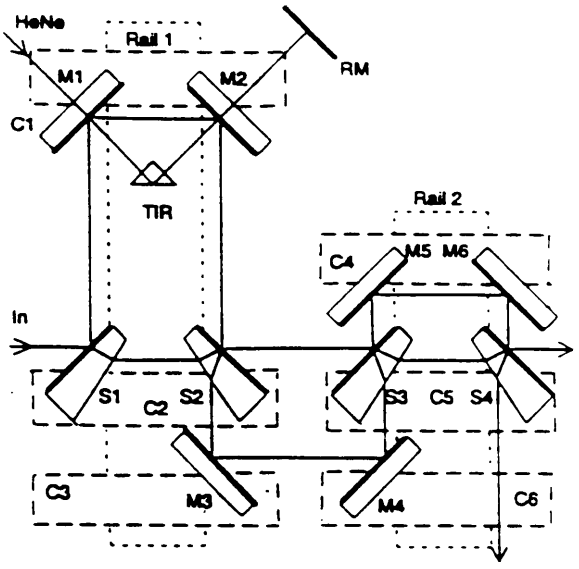

Figure 4: Schematic diagram indicating how the beam splitters, S1 to S4, and mirrors M1 to M6 of fig.(1)a are mounted on carriages C1 to C6 and rails. Heavy lines denote the actual mirror and beam splitter coatings. Reference mirror RM and the TIR prism required for geometrical alignment are shown.

The first step is to ensure that the alignment beam is aligned at 45° with respect to the bare rails on which the generator is to be mounted. A TIR prism, which is mounted from a gantry so that it does not interfere with the displacment of carriages along the rail, and then the reference mirror (RM) are inserted into this beam and their reflections (or fringe patterns if visible) aligned onto the pinhole screen shown in figure (3). Carriage C1 is now placed on the rail, and with M1 removed from its mount, slid along the rail until M2 encounters the alignment beam as shown in figure (5)a. M2 is then aligned with respect to RM by observing the Tolansky fringes produced between the two optics in either transmission on screen S or in reflection on the pinhole screen PS. It is only necessary to observe one fringe pattern. Carriage C2 is then slid into place with S1 only in its mount as shown in fig.(5)b and S1 aligned with respect to M2. In this case the fringes are observed either on a screen S placed between M2 and RM or on the pinhole screen PS. S2 is now placed in its mount, fig.(5)c, and aligned with respect to S1. The distance between M2 and RM is sufficiently large to allow M2 to be slid conveniently out of the way without interfering with RM and so permit clearer observation of the S1/S2 transmission fringes. M2 can always be realigned with respect to RM. Having aligned S1 and S2 carriage C2 is removed from the rail and M1 aligned with respect to M2, fig.(5)d. M3, mounted on carriage C3, may now be aligned with respect to M1 as shown in fig.(5)e. The optics for rail 1 are now geometrically aligned and are removed from the rail. The optics to be mounted on rail 2 are similarily aligned on rail 1 using the TIR

and the RM as references as before.

Which optic is aligned with respect to which and the order (which is not unique) of alignment in the procedure described is such that (1) the beam path length between any two optics being aligned is the same (to within a centimeter or so) and (2) the alignment beam does not traverse any other mirrors or splitters prior to the pair being aligned. The first point ensures that the alignment beam need only be optimized once, thereby providing a single reference, to achieve geometrical alignment of all the optics of the generator. For example having optimized the parameters of the alignment beam so that the Tolansky fringes generated between optics separated by alignment beam path of 24cms, eg M1 and M2, the same beam will not permit the clear observation of fringes between optics close together as would be the case if one were to try to align S1 with respect to M1 for example. The second point ensures that the visibility of the fringe systems produced by the optics being aligned is not reduced due to the presence of an additional optic in the beam or confused due to the observation of other fringe patterns.

The visibility of the fringes is a function of the reflectivies of the reflecting surfaces as well as the distance between them. In the CTF a yellow HeNe (594nm) alignment beam was used since the 209nm beam splitter coatings used had a reflectivity of about 50% at this wavelength. The

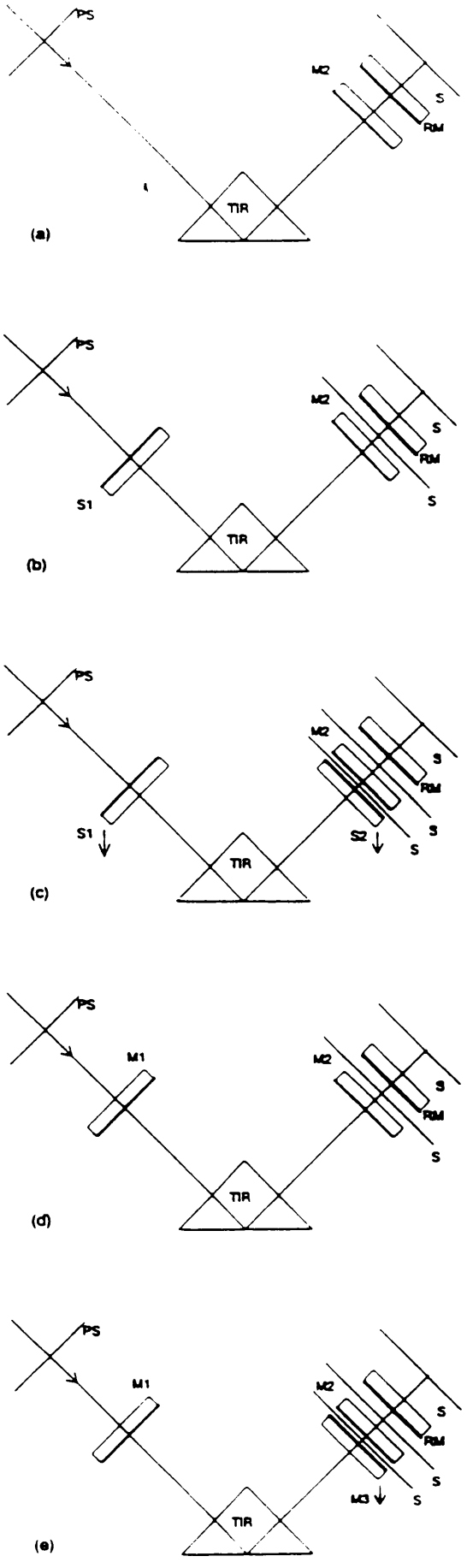

Figure 5: Schematic illustrating a geometrical alignment procedure for the optics mounted on rail 1 of fig.(4). Nomenclature as before with the addition of S denoting screen and PS denoting pinhole screen (see text).

high reflectivity mirrors were undercoated with an adjusting layer the effect of which was to provide a reflectivity of more than 70% at 594nm. The mirrors and splitters used in the generator are required to have very parallel substrates so as to avoid the confusing observation of more than one fringe system from each substrate.

To render the Tolansky fringes observable and achieve a high degree of accuracy the point source of fig.(3), at which the pinhole screen is located, was placed 2.5m away from the surfaces to be aligned. A TIR prism with a prism angle good to 2 secs of arc was used. Figure (6) provides an overview of the synchro-laser, and of the PTG and its alignment optics. In the PTG constructed the distance between the two mirrors of a stage (and therefore also between the two splitters) was set at 170mm such that the optics to be aligned parallel to each other were approximately 240mms apart in the alignment beam. Thus, from eqn.(1), assuming that the fringe pattern may be centered to within a 1mm, it should be possible to align the surfaces parallel to each other to an accuracy of approximately three seconds of arc when viewing the fringe patterns in reflection.

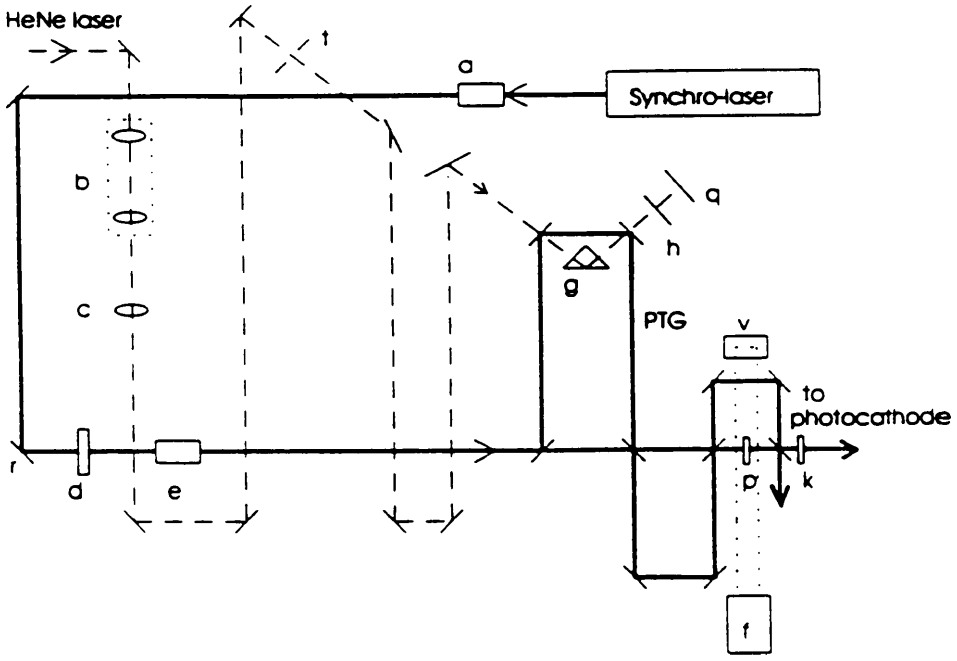

Figure 6: Overview of the synchro-laser and of the PTG and its alignment optics. Heavy line indicates the path of the synchro-laser with Galilean telescope (a), $\lambda/2$ waveplates (d) and (p), Rochon prism (e) and $\lambda/4$ waveplate (k). Broken line indicates the HeNe alignment beam used for geometrical alignment with collimator (b), 2.5m focal length lens (c), pinhole screen (t), TIR prism (g), reference mirror (h) and screen (q). Dotted line shows interferometer (f) beam line along rail 2 of the PTG, reflector optic (v) only shown. Correct injection of the synchro-laser pulse into the PTG is ensured using mirror r. (Taken from [1])

To ensure that on correct injection of the main synchro laser pulse into the PTG that the pulses generated travel parallel and perpendicular to the axis of the rails along which the stage lengths are measured, the HeNe alignment beam itself should be aligned at 45° to the axis of the rails. In order to achieve this two short rails are mechanically aligned along an axis that makes an angle of 45° to the generator rails, already aligned parallel to each other. Using an iris, mounted on a carriage which may be positioned on both of these alignment rails, the alignment beam can be optically decoupled along this axis. The accuracy of this alignment is not critical. For a correctly aligned generator into which the main laser pulse is well injected an alignment error of the HeNe beam, $\Delta\Theta_{HeNe}$, will introduce a stage timing error of $2 * l/cos(\Delta\Theta_{HeNe})$ were l is the stage length. Therefore in a stage of length 208mm say, an alignment error of $\Delta\Theta_{HeNe} = 0.5°$ will introduce a stage timing error of only 0.05ps. Alignment accuracies of 0.5° are easily achievable using standard optical decoupling.

3 Timing

3.1 Principle

The timing between pulses is determined by the distances between the mirror and splitter coatings of the various stages. To set these distances reflecting surfaces, already aligned parallel to each other, are brought close together until the distance between them may be taken to be negligible. When this t=0 distance has been set one surface is displaced a known distance with respect to the other.

The t=0 distances may be set either by visual inspection or by viewing Tolansky fringes in transmission. As the distance between the surfaces is reduced the diameter of the Tolansky fringes, will be observed to grow. The angular diameter ϕ_p of the p^{th} fringe is given by

$$\phi_p = \sqrt{\frac{4p}{t}} \tag{3}$$

where t is the distance between the surfaces [5]. In an optimized alignment beam it should be possible to set the separation of the surfaces accurately without allowing them to touch. If the aligment beam is not sufficiently optimized an estimation of the surface separation may be obtained by observing the relative displacement of the Tolansky fringes when the optics are allowed to lightly push against each other. In this case an abrupt displacement of the centre of the fringe system will be observed when one optic begins to push against the other.

Having set the t=0 settings between two optics one is displaced a known distance with respect to the other. This distance is measured parallel to the rail along which the interferometer has been aligned and perpendicular and parallel to which the generated pulses travel.

3.2 Procedure for setting the stage timings

To demostrate how the technique described above may be used to set the timing within a generator a procedure for rail (1) of figure (4) is presented. It can be seen from figure(4) that it is not possible to set the stage length between S2 and M3 by bringing their reflecting surfaces into contact. To set the length of this stage, M3 is brought into contact with M2 and displaced a distance equal to the sum of the two stage lengths. The length of stage 1 is then set.

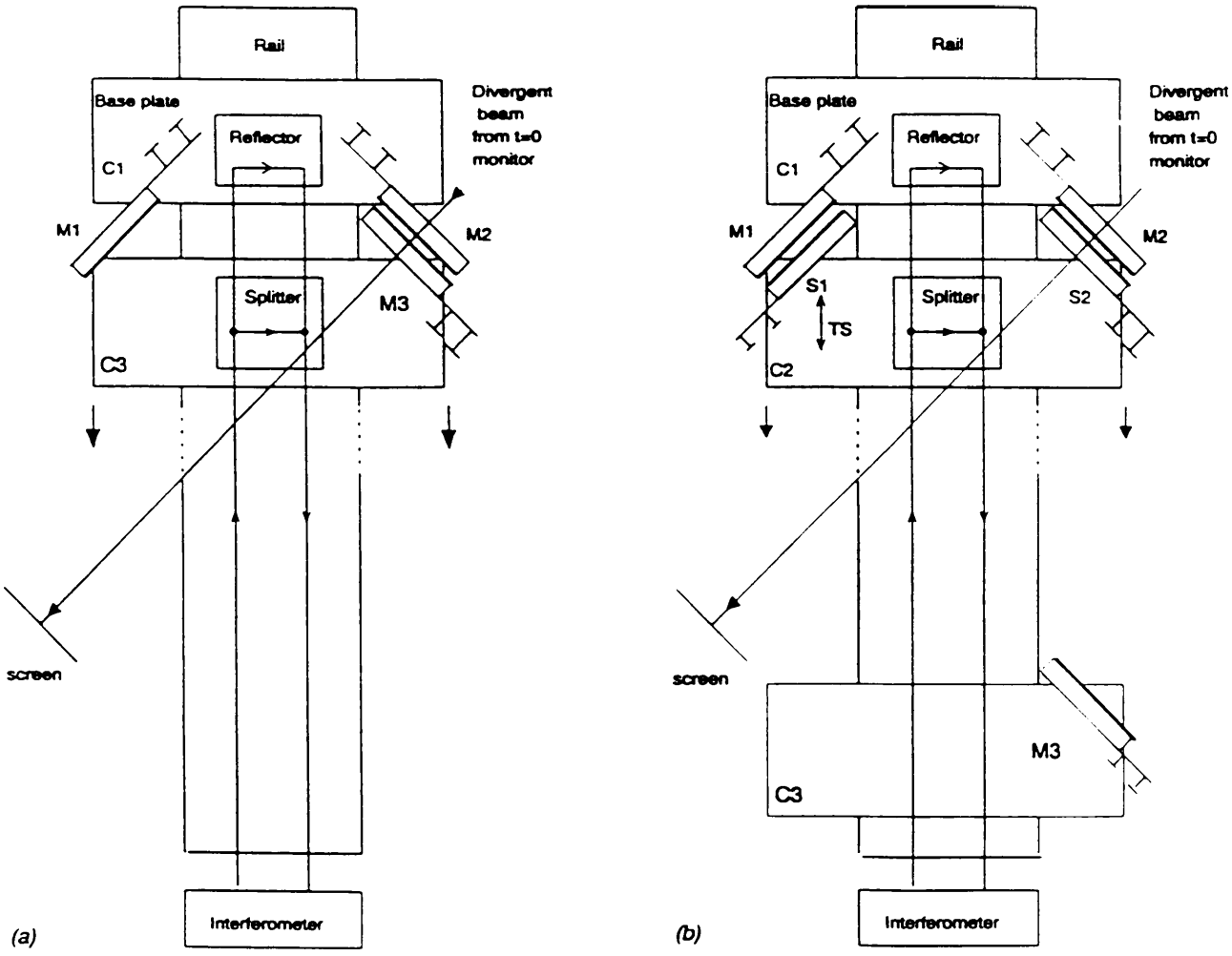

Figure 7: Schematic illustrating the procedure for setting the timing between optics mounted on rail 1 of fig.(4). (a) indicates how the M2/M3 separation is set, (b) shows how the timing of stage 1 is set.

The first step is to align the interferometer parallel to the axis of the rail. Since it is the M2/M3 distance which must be set first the interferometer beam splitter optic is placed on carriage C3, as shown in figure (7)a and the beam aligned in the normal way by means of optical decoupling. Carriage C1 is then fixed at some convenient location on rail 1, and the interferometer reflector optic mounted on it and aligned. M1 and M2 are now the references with respect to which all other optics are displaced. Fig.7(a) shows the t=0 distance being set between M2/M3. Carriage C3 is positioned so that M2 and M3 are close together. The translational stage, mounted beneath the base plate of carriage C3 (not shown on the diagram) is adjusted to set the t=0 distance and the interferometer reading set to zero. Carriage C3 is then displaced the required distance by simple sliding the carriage along the rail. The separation of the optics may be fine tuned using the same TS mounted beneath the carriage base plate. Figure 7(b) shows C3 at its required distance from C1. Carriage C2 is now placed on the rail. The interferometer beam splitting optic is removed from C3, placed on C2 and aligned with respect to the interferometer beam. The M2/S2 t=0 distance is set using the translational stage supporting carriage C2. To do this freely S1, which is mounted on an additional TS, must be retracted so that it does not come into contact with M1 while the S2/M2 distances is being set. After having set the S2/M2 t=0 distance, the t=0 monitor is placed behind M1 and the S1/M1 t=0 distance set solely by adjusting the TS on which S1 is mounted. Having set both t=0 distances, C2 may be slid along the rail to achieve the required stage length. Fine adjustments to the stage length are made using the TS mounted beneath the carriage base plate. Rail 2 is similiarly aligned with the M5/M4 separation set first and then the timing of stage 3.

The HeNe alignment beam used to geometrically align the optics can not be used to set the t=0 settings as the fringe patterns it would produce between two optics placed very close together would have fringes of very large diameter. Instead a more highly divergent beam is required. Presented in figure (8) is an example of such a system. The system is compact and portable so that it may be easily transferred from one side of a rail (to set the M2/S2 t=0 for example) to the other (to set the M1/S1 t=0).

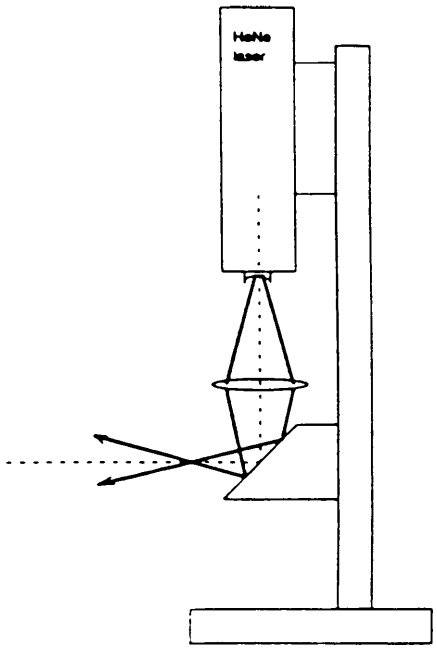

Figure 8: Schematic of compact t=0 monitor

3.3 Stage length calculations

For a 'top stage' configuration, see fig.(9) the delay Δ between two pulses at the output of the stage is be given by

$$\Delta = (2t_t + 2t_a + t_c) - (2t_s + t_c) \quad (4)$$

where t_t, t_c, t_a, and t_s are the times it takes for a light pulse to travel the distances l_t, l_c, p_a, and p_s as shown. The transit time T of a pulse along a path lenght L is calculated using the group velocity u which is related to the velocity of light c in vacuum by c/n' where n' is the group refractive index. Thus

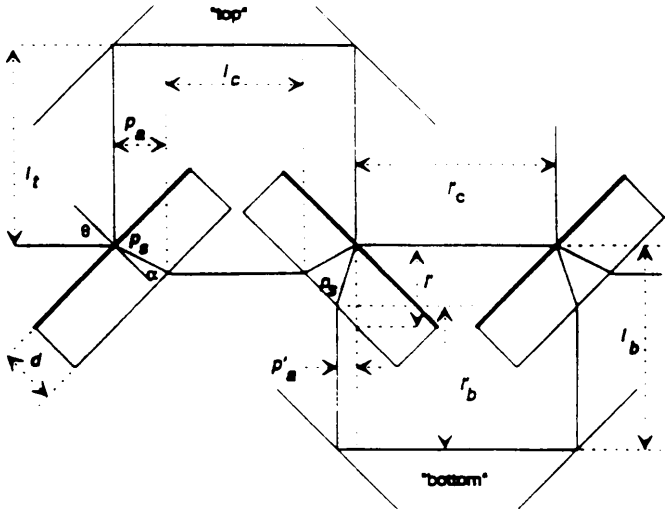

Figure 9: Nomenclature used in stage length equations (see text).

$$T = \frac{L}{u} = \frac{Ln'}{c}. \quad (5)$$

Rearranging eqn.(4) and writing $t_t = ln'_a/c$, where n'_a is the group refractive index of air, yields

$$l_t = \frac{c}{n'_a}\left\{\frac{\Delta}{2} + t_s - t_a\right\} \quad (6)$$

To calculate the transit time t_s of the pulse through the substrate the phase velocity is used to calculate the path length and the group velocity to calculate the transit time of the pulse energy along this length. Thus the path length p_s is given by

$$p_s = \frac{d}{cos\alpha} \quad (7)$$

where d is the thickness of the substrate matieral and α is the angle of refraction seen by the pulse as obtained using Snells law

$$n_a sin\theta = n_s sin\alpha \quad (8)$$

θ being the angle of incidence and n_a and n_s respectively the phase refractive indices of air and fused silica at the wavelength under consideration. From simple trigonometry eqn.(7) becomes

$$p_s = \frac{d.n_s}{\sqrt{n_s^2 - n_a^2 sin^2\theta}}, \quad (9)$$

thus

$$t_s = \frac{d.n_s}{c\sqrt{n_s^2 - n_a^2 sin^2\theta}}.n'_s \quad (10)$$

where n'_s is the group refractive index in the substrate. For the case of a PTG, where the angles between the desired beam paths and the normals to the optics are at 45° and it is the beam path into the system which is rotated to obtain correct injection (see reference [2] for converse case where the beam path is fixed and it is the optics which are rotated), p_a is written

$$\begin{aligned} p_a &= p_s.cos(45-\alpha) \\ &= \frac{d}{\sqrt{2}}\left\{1+\frac{n_a sin\theta}{\sqrt{n_s^2-n_a^2 sin^2\theta}}\right\} \end{aligned} \tag{11}$$

yielding

$$t_a = \frac{d}{c\sqrt{2}}\left\{1+\frac{n_a sin\theta}{\sqrt{n_s^2-n_a^2 sin^2\theta}}\right\} n'_a \tag{12}$$

Eqns.(10) and(12) are general with respect to angle of incidence and are only meaningful with respect to the stage length l_t, required to generate a time delay Δ, when evaluated at θ=45° thereby yielding from eqn.(6)

$$l_t = \frac{\Delta.c}{2n'_a} + \frac{\sqrt{2}.d}{\sqrt{2n_s^2-n_a^2}}\left\{\frac{n_s n'_s}{n'_a} - \frac{1}{2}\left\{\sqrt{2n_s^2-n_a^2}+n_a\right\}\right\} \tag{13}$$

The delay Δ between two pulses at the output of a 'bottom stage' is given by

$$\Delta = 2t_b + 2t'_a + 2t_s + t'_c - t'_c \tag{14}$$

yielding

$$l'_b = \frac{c}{n'_a}\left\{\frac{\Delta}{2} - t_s - t'_a\right\} \tag{15}$$

where t'_b, t'_c, t'_a, and t_s are the times it takes for a light pulse to travel the distances l'_b, l'_c, p'_a, and p_s as shown in figure xx. Recalling that in the alignment procedure it is the distance between reflecting surfaces which is measured the length of a 'bottom' stage is given as

$$l_b = l'_b + l' \tag{16}$$

where

$$l' = \sqrt{2}.d \tag{17}$$

Thus for example the distance between M3 and M2 of fig.7(a) is set to $l_t + l_b$. In a 'bottom' stage configuration p'_a is given by

$$\begin{aligned} p'_a &= p_s.sin(45-\alpha) \\ &= \frac{d}{\sqrt{2}}\left\{1-\frac{n_a sin\theta}{\sqrt{n_s^2-n_a^2 sin^2\theta}}\right\} \end{aligned} \tag{18}$$

yielding

$$t'_a = \frac{d}{c\sqrt{2}} \left\{ 1 - \frac{n_a sin\theta}{\sqrt{n_s^2 - n_a^2 sin^2\theta}} \right\} n'_a \tag{19}$$

Thus

$$l_b = \frac{\Delta.c}{2n'_a} - \frac{\sqrt{2}.d}{\sqrt{2n_s^2 - n_a^2}} \left\{ \frac{n_s n'_s}{n'_a} + \frac{1}{2} \left\{ \sqrt{2n_s^2 - n_a^2} - n_a \right\} \right\} + \sqrt{2}.d \tag{20}$$

The expressions for l_t and l_b derived here assume that the beam splitter substrates are of zero wedge angle, i.e. that the front and back surfaces are prefectly parallel to each other. To evaluate the stage lengths one must know the group and phase refractive indices of air and the substrate matieral at the desired wavelength. The expressions and optical constants required to evaluate these indices are given in reference[2]. In this reference it is also shown that in the ultraviolet region of the spectrum that the group refractive index of synthetic fused silica, the substrate matieral, may not be neglected, i.e. assumed equal to the phase refractive index, without introducing timing errors of the order of some picoseconds for a 9.24mm thick substrate.

4 Injection

To access injection error one requires a stage (constructed using beam splitter optics of sufficiently small wedge angle, see §5) which has been geometrically aligned and in which the t=0 settings have been made. The latter guarantees, for example, that the separation of the reflecting surfaces of S1/S2, cf fig.(4), is equal to that between those of M1/M2 and so ensures that the situation illustrated in fig.(10) can not arise.

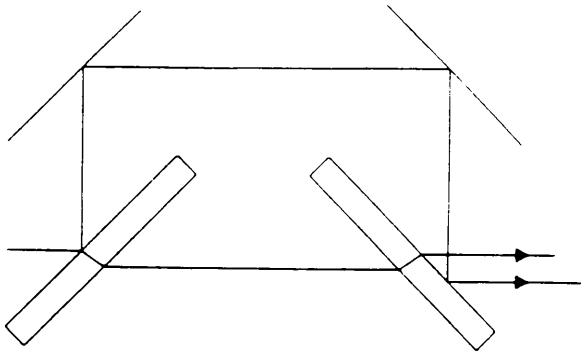

Figure 10: Stage in which the distance between the reflecting surfaces of the beam splitter optics (thick oblongs) is not equal to that between the mirrors (thin lines). As a result, although the stage is otherwise correctly aligned and the input pulse injected at exactly 45°, the two output pulses emerge travelling parallel but separate paths.

If the stage is correctly aligned but the beam injected with an error of $\Delta\Theta$ then the two output pulses will be found to travel parallel but separate paths as indicated in fig.11(a) and will appear on a screen placed at, or a few centimeters from, the stage output as shown in fig.(11)b. The injection error is corrected by rotating the path of the input laser pulse so that the two output pulses coincide see fig.(11)c. This is achieved by rotating mirror (r) of fig.(6) with the waveplate (d) and polarizer (e) removed.

Fig.(12) is a plot of beam separation in mms (measured on a screen at right angles to the desired beam path and placed immediately at the stage output) against the injection error angle $\Delta\Theta$, given in seconds of arc, and illustrates that the accuracy to which $\Delta\Theta$ may be set is a function of stage length. With the naked eye one can easily determine beam separation to within 0.5mm. Thus using a stage length of 600mms the injection angle could be set to approximately 8.5 seconds of arc producing timing errors of 0.6ps and 0.14ps in stages of lengths 208.9568mm and 58.9301mm respectively as shown in fig.(13). Beam separations of the order of 0.5mm are easily observed in the laboratory. With increased operator skill, or by using longer stage lengths, or by using a more precise method other than that of visual inspection

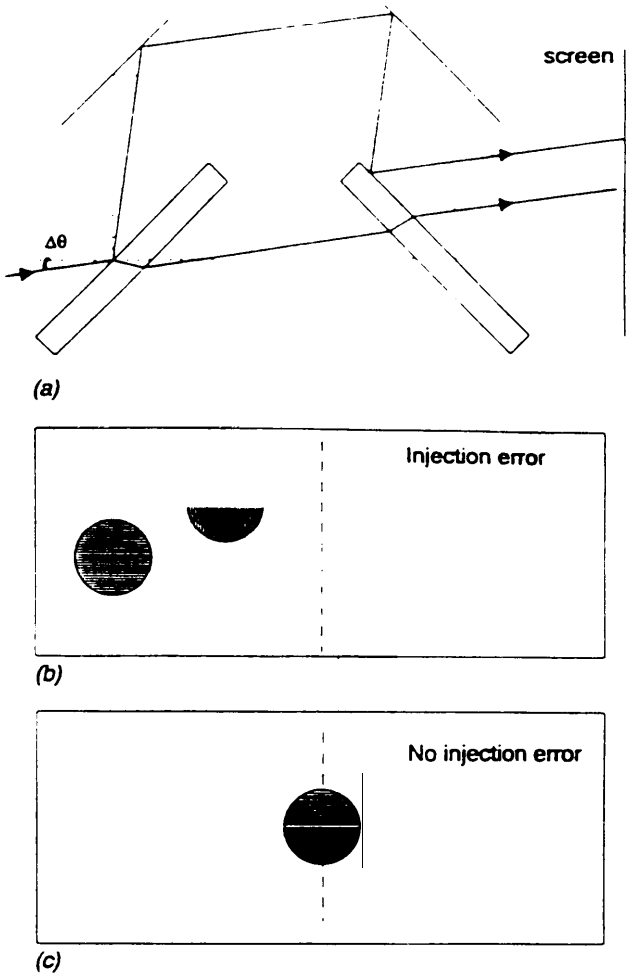

Figure 11: (a) Paths taken by the two pulses generated at the input splitter to the stage for the case where the input pulse has been injected with an error of $\Delta\Theta$. (b) Appearance of the two output pulses on a screen placed at, or a few centimeters from, the stage output. In this case a piece of card has been inserted between the two beam splitters to obscure one half of the straight through beam and so provide the semicircle shown. (c) On correction of injection error, through the use of mirror r of fig.(6), the two beams will overlap as shown.

to initially correct error much better accuracies should be obtainable.

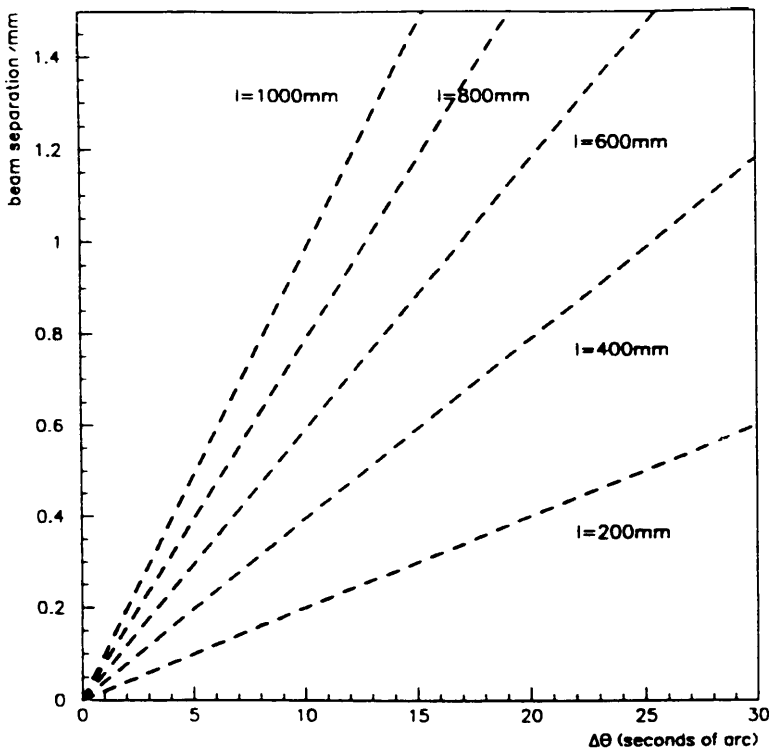

Figure 12: Plot of beam separation, measured on a screen placed immediately at the stage output, see figure 11(a), as a function of injection error $\Delta\Theta$ for different stage lengths l_t (Distance between centres of stage mirrors is 170mm.)

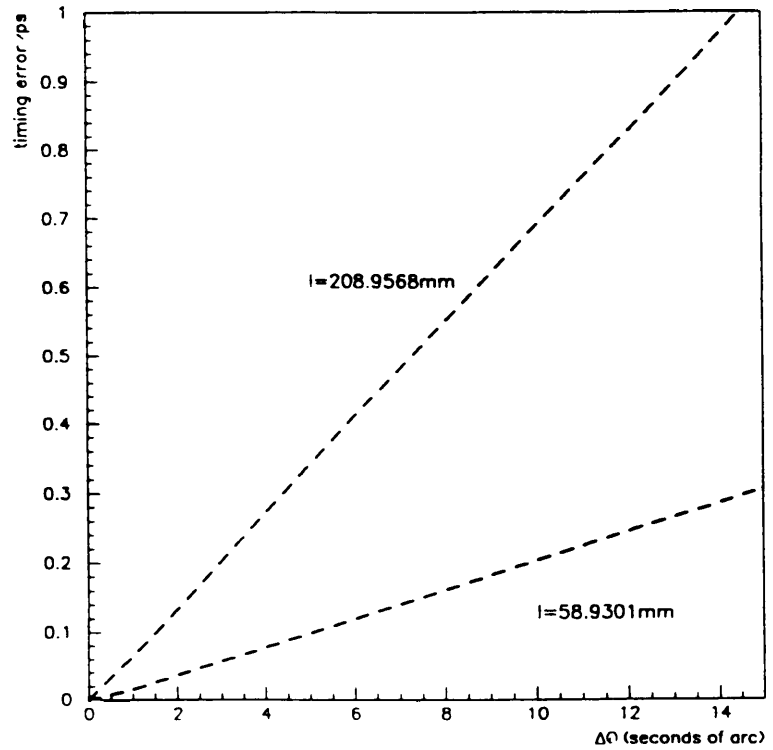

Figure 13: Plot of the timing error that would be introduced into stage lengths of l_t=208.9568mm and l_t=58.9301mm as a function of injection error $\Delta\Theta$.

In those cases where the required length of the longest stage will enable $\Delta\Theta$ to be set with the accuracy required the beam injection can be set after the PTG timing has been set. If longer stage lengths are required to achieve the desired accuracy the injection should be set prior to setting the stage timings.

Once the injection has been correctly set any additional alignment error observed on a distant photocathode is the product of either small alignment errors within the stage itself, or due to small deviations in the parallelism of the rail on which the carriages are mounted or due to problems of carriage location. These errors are investigated by looking at the individual stage outputs in turn. In practise they were found to be small, of the order of 11 sec of arc, and so may be easily corrected for by adjusting the second detour mirror encountered in the stage. The timing error introduced by this adjustment is negligible.

In addition to the generation of timing errors poor injection will determine the degree of coincidence acheived between the pulses of the train at a distant photocathode. For example although an estimate of beam separation accurate to 0.5mm may be sufficient with respect to the timing accuracies required the degree of coincidence between any two pulses on the photocathode will only be good to within 0.5mm.

5 Influence of wedge angle

The achievable degree of coincidence of pulses on a distant photocathode is limited by the wedge angle of the splitter substrates. This is demonstrated here by considering a perfectly aligned stage in which the beam splitters are orientated, with respect to wedge angle, in either one of the configurations presented in fig.(14). The separation of the two output pulses and the angular divergence between their beam paths was computed, cf table 1, for different values of wedge angle assuming that the input pulse is injected at exactly 45°.

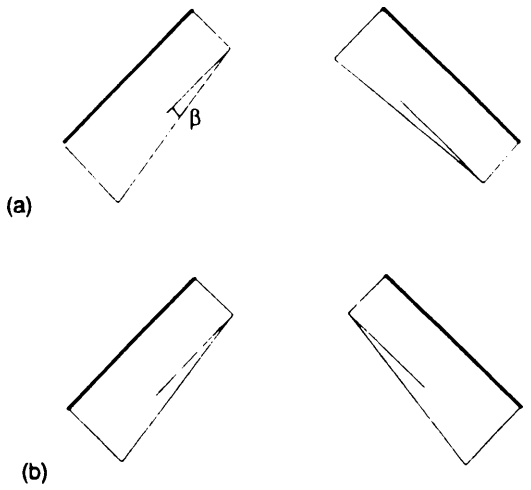

Figure 14: Orientations of beam splitters with respect to their substrate wedge angle β for (a) configuration a and (b) configuration b.

Beam separation (at the output) is the first indication of the degree of coincidence achievable on a distant photocathode. From table 1 one can see immediately that if pulse coincidence of $20\mu m$ or less are required the wedge

wedge	Configuration a		Configuration b	
angle	divergence/deg	separation/mm	divergence/deg	separation/mm
5 mins	$3x10^{-4}$	0.198	0.1554	0.215
2 mins	$5x10^{-5}$	0.079	0.0622	0.086
30 secs	$3x10^{-6}$	0.020	0.0155	0.021
10 secs	$4x10^{-7}$	0.006	0.0052	0.007
5 secs	$9x10^{-8}$	0.004	0.0026	0.004
2 secs	$1.4x10^{-8}$	0.001	0.0010	0.001

Table 1: Separation of pulses and the angular divergence of their beam paths as a function of substrate wedge angle for configurations (a) and (b) of fig.(14)

angles of 30 secs or less should be used. For the configuration (a) orientation beam path divergence is negligible and pulses will be coincident on the photocathode to $6\mu m$ or less for optics of wedge angle of 10 secs or less. To achieve such accuracies one must (1) be able to set injection to the same accuracy and (2) be able to mount the optics accordingly i.e. to determine the orientation of the wedge. If μm accuracy is not required one can mount the optics without knowledge of wedge orientation and risk the 'worst case' corresponding to configuration (b). For this configuration the divergence of the beam paths is no longer negligible and for a three stage generator of fig.1(a) one can expect the eight pulses generated to hit the photocathode at slightly different locations. The pulse which is reflected at all four beam splitters arrives at the photocathode without experiencing the effect of beam splitter wedge angle. Using this pulse as the reference pulse the relative displacements of the other seven pulses on arrival at a photocathode, located 20m away from the output of the generator, were calculated and the maximum displacements listed in table 2. From table 2 it can be seen that if the pulses are required to be coincident to within 0.7mm then splitters of 2 secs of arc wedge angle should be used.

Wedge Angle secs of arc	Maximum pulse separation/mm
30	10.8
10	3.6
5	1.8
2	0.7

Table 2: Calculated maximum pulse separation expected at a photocathode 20m from the output of a PTG of the type illustrated in fig.(1)a.

The technique described in §4 to set the injection angle assumes that the beam separation at the stage output is a function of injection angle only. This can only be assumed if the wedge angle contribution to beam separation is negligible with respect to the accuracy with which the injection angle is required to be set. Large wedge angles are therefore not to be recommended. Wedge angle should be kept as small as possible since not only will injection angle determination and pulse coincidence on the photocathode be effected but the geometrical alignment technique described in §2 will be complicated due to the visibility of fringe patterns generated by the front and back surfaces of individual substrates.

When using small wedge angle substrates one must ensure that the substrates are sufficiently thick with respect to the main laser pulse width to avoid interference effects.

6 Experimental results

A PTG was set up to generate a train of eight pulses of separation 333.49ps at 209.42nm. The t=0 settings were set by visual inspection. The timing was tested by measuring the time interval between pairs of consecutive pulses, i.e. between pulses 1 and 2, 2 and 3 etc, using a streak camera and was found to be good to within 3ps. The resolution of the streak camera is given as 2ps across the central portion of the 576 pixel image provided. However since the pulse separation is such that the two pulses always lie outside this central region a recorded accuracy of 3ps is good and still within the accepted resolution of the camera for an image not contained within the central area. If the stage timing error is taken to be e then the maximum relative timing error that can occur in a three stage generator is of magnitude $3e$ and occurs where errors of $-e$, $+e$, and $+e$ occur in stages 1,2 and 3 respectively. If the maximum relative error has been induced then from the results one can say that a stage error of 1ps or better has been achieved. In practise, since it is not the entire stage paths that are measured but only the detour lengths, one can say that the method of setting the timing is accurate to 500fs. The minimum relative stage error that can occur is $1e$ and corresponds to a stage length timing accuracy of 1.5ps.

In early tests a generator of the type illustrated in fig.(1)a was constructed using three beam splitters of 2 secs of arc wedge angle and with an unoptimized optic of undetermined wedge angle known to be greater than 10 secs of arc. Optics were aligned without knowledge of wedge angle orientation and the pulses were found to be coincident to within 1.5mm of each other on the photocathode 20m from the PTG output. This would be expected if the output optic were to have a wedge of 10 secs. In later tests, using four beam splitters of 2 sec of arc wedge angle and thickness 9.24mm, the eight pulses

were observed, by visual inspection, to be coincident at a distance of 20m from the PTG output.

7 Concluding remarks

Calculations based on the vectorial additional of the 30GHz field contributions from the individual electron pulses generated by a train of laser pulses indicate that both the cumulative timing error and the relative error between any two consecutive pulses should be less than 2ps. Assuming timing errors of equal magnitude e per stage, a stage timing error of $e \leq \frac{2}{3}$ps, or a stage length timing error of $e_l \leq \frac{1}{3}$ps is thus required. With an effective streak camera resolution of 3ps it is only possible to say that if the maximum relative stage error has been incurred then the technique has a stage length timing accuracy of better than 500fs. However if the minimum relative error has been incurred the stage length timing accuracy could be of the order of 1.5ps.

The eight pulses of the train were found on visual inspection to be coincidence (to better than 1mm) 20m from the PTG output. This was achieved without knowledge of the wedge orientation of the individual splitters and by setting the injection by visual inspection. It has been shown computationally that if care is taken with respect to wedge orientation then μm alignment accuracies between the pulses at a distance of 20m from the PTG output should be attainable provided that some method of achieving injection accuracies of the same order is availible.

Acknowledgements

The author would like to acknowledge the contribution of Pierre Joly who recognized that the effective refractive index of approximately 1.8 of the fused silica beam splitter substrates that appeared to be responsible for timing errors in the PTG constructed was in fact the group refractive index of the substrate matieral at 209nm.

References

1. P.M. Devlin-Hill, *Pulse train generation at 209nm.*, CERN PS 93-40(LP) and CLIC Note 209. Paper presented at the Workshop on High Intensity Electron Sources., Legnaro, Padova, Italy 1993.

2. P.M. Devlin-Hill, P. Joly, *Delay time experienced by a laser pulse on transit through a substrate.* CERN PS 94-05(LP)

3. T.G. Bergman, J.L. Thompson, *An Interference Method for Determining the Degree of Parallelism of (Laser) Surfaces,* Appl. Opt., 7, 923 (1968).

4. D.L. Ford, J.H. Shaw, *Rapid Method of Aligning Fabry-Perot Etalons*, Appl. Opt., **8**, 2555 (1969).

5. D. Malacara, *Optical Shop Testing*, John Wiley and Sons, New York, 1978.

6. S. Tolansky, *Multiple-Beam Interferometry of Surfaces and Films*, Dover, New York, 1970.